



The Pulsed Flame Photometric Detector for analysis of phosphorus pesticides in wastewater and food commodities

Application Note

Environmental

Authors

Agilent Technologies, Inc.

Introduction

Twenty-eight elements can be detected with the PFPD, thirteen of which give delayed emissions, and therefore infinite selectivity. These latter elements include environmentally and industrially important S, P, As, Sn, and N.

Phosphorus is one of the most sensitive elements detected by the PFPD (P-PFPD) with a detectivity of 0.1 pg/s, a linear dynamic range of 10^4 , a 10^6 selectivity versus carbon, and a high selectivity versus S. This makes it an ideal detector for the analysis of organophosphorus pesticides (OPP) in analytical extracts from waste water and agricultural products.

The PFPD has advantages over the other two phosphorus sensing GC detectors: 1) the Thermionic Specific Detector (TSD), a nitrogen-phosphorus detector, and 2) the Flame Photometric Detector (FPD). Comparisons are made between these detectors. Finally, high speed data acquisition firmware and software that allows one to easily set up the PFPD and review the pulsed emission data emanating from each chromatogram is described.



Agilent Technologies

Experimental

In a conventional flame photometric detector (FPD), a sample containing heteroatoms of interest is burned in a hydrogen-rich flame to produce molecular products that emit light (i.e. chemiluminescent chemical reactions). The emitted light is isolated from background emissions by narrow bandpass wavelength-selective filters and is detected by a photomultiplier and then amplified. The detectivity of the FPD is limited by light emissions of the continuous flame combustion products including CH^* , C_2^* , and OH^* . Narrow bandpass filters limit the fraction of the element-specific light which reaches the PMT and are not completely effective in eliminating flame background and hydrocarbon interferences. The solution to this problem, was to set the fuel gas (H_2) flow into the FPD so low that a continuous flame could not be sustained. But, by inserting a constant ignition source into the gas flow, the fuel gas would ignite, propagate back through a quartz combustor tube to a constriction in the flow path, extinguish, then refill the detector, ignite and repeat the cycle. The result was a pulsed flame photometric detector (PFPD) shown in Figure 1.

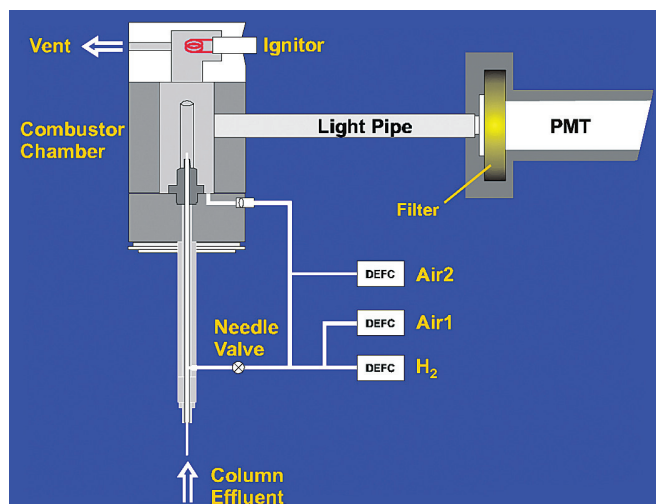


Figure 1. Schematic Cross Section of the PFPD

Phosphorus Sensing Detectors

The background emissions from the hydrogen-rich air: hydrogen flame (approximately 10 mL/min H_2 and 40 mL/min air) is a broad-band chemiluminescence. The combustion of hydrocarbons is highly exothermic, rapid and irreversible, producing a light emission equal to the time for the flame to propagate through the combustor, or 2 to 3 milliseconds. Many of the chemiluminescent reactions of other elements such as S (S_2^*), P (HPO^*), N (HNO^*) etc., are less energetic and more reversible, and proceed after the temperature behind the propagating flame has dropped. These heteroatom emissions are therefore delayed from the background emissions. By using the leading edge of the flame background emission to trigger a gated amplifier with an adjustable delay time, heteroatom emissions can be amplified to the virtual exclusion of the hydrocarbon background emission. This selective amplification of the element-specific emissions is the basis of the PFPD's unique sensitivity and selectivity (see Figure 2).

The PFPD pulses approximately 3 to 4 times per second so that in a period of about 250 to 330 milliseconds the detector fills with the mixture of fuel gases and column effluent. When the flame propagates through this mixture, all the light emission from a given flux of some element, for example, phosphorus, is concentrated into a period of only 10 milliseconds following each flame pulse. This light intensity is approximately 30 times brighter than the steady state emission from a conventional FPD where the emission would be spread over a period of 330 milliseconds. This effect plus the fact that the gated amplifier is only active during a 10 millisecond period for phosphorus combines to greatly improve the signal to noise ratio in the PFPD.

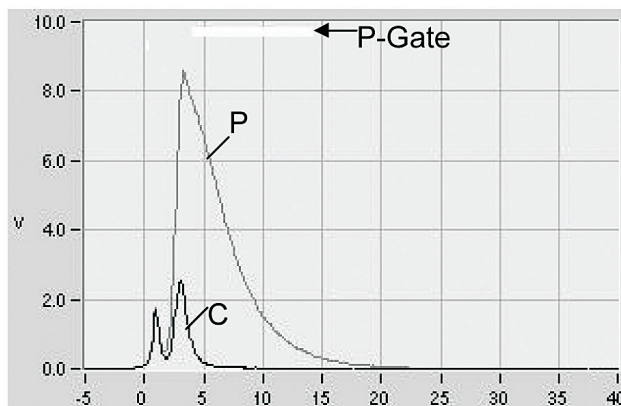


Figure 2. Flame Background and Phosphorus Emission Time Profiles

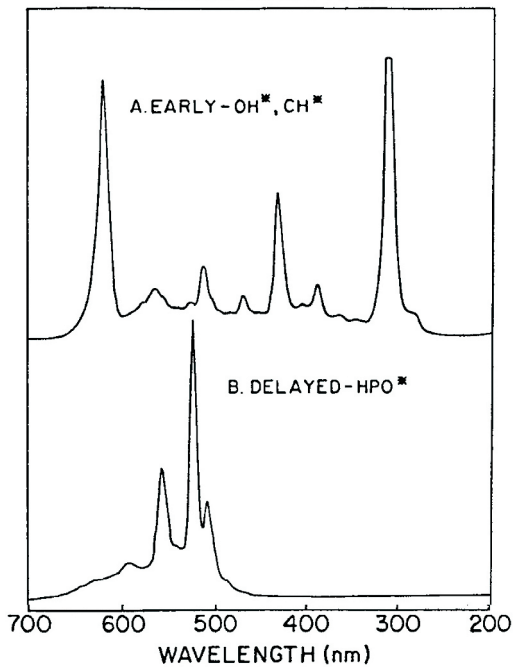


Figure 3. Hydrocarbon and Phosphorus Emission as a function of Wavelength. Filter used for P is the GG-495.

Phosphorus Sensing Detectors

The delayed phosphorus or sulfur emissions are integrated after the flame background has dropped to a negligible level. This delay permits the use of much wider bandpass optical filters that no longer must filter the background but can be selected to target the wavelength range of the desired element-specific emissions (Figure 3). This results in a lower overall noise level and greater detectivity.

The PFPD detects 28 elements:

S, P, N, C, As, Sn, Se, Mn, B, Br, Ga, Ge, Pb, Si, Te,
V, Al, Bi, Cr, Cu, Eu, Fe, Ni, Rh, Ru, W, In, Sb

Thirteen of these elements have delayed emissions from the background carbon emission and therefore exhibit infinite selectivity:

S, P, N, As, Se, Sn, Ge, Ga, Sb, Te, Br, Cu, In

Control of the PFPD parameters is either from the GC or the workstation (Figure 4).

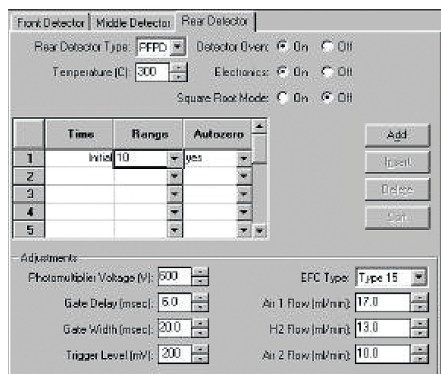


Figure 4. Workstation Control of PFPD

Phosphorus Sensing Detectors

The phosphorus detectivity of the P-PFPD is 0.1 pg/s and the selectivity versus carbon is 10⁶. This detectivity is the same as the TSD or NPD detectors, but the PFPD produces peaks without tailing and has better selectivity towards hydrocarbons and nitrogen compounds. Figure 5 compares the PFPD and TSD for five phosphorus pesticides. The greater selectivity for the PFPD is apparent from the smaller solvent response and relatively low baseline noise and drift.

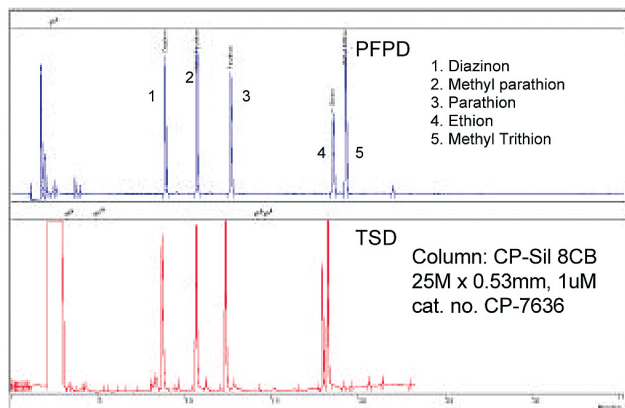


Figure 5. PFPD & TSD (NPD) for Phosphorus Pesticides

The detectivity and selectivity of the P-PFPD are 10 fold better than the FPD. A pesticide extract that contains a high degree of sulfur interference is shown in Figure 6a (PFPD) and 6b (FPD). The greater selectivity of the P-PFPD is apparent from this comparison.

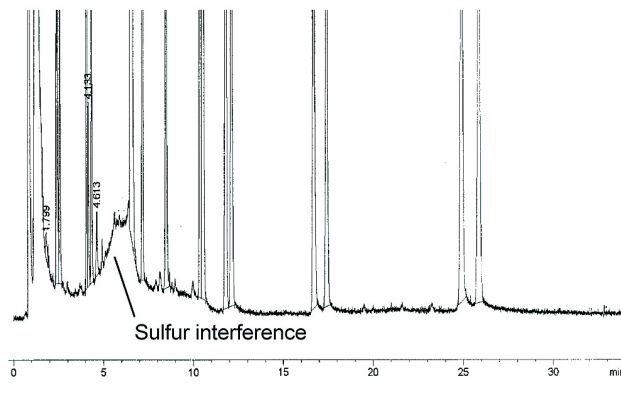
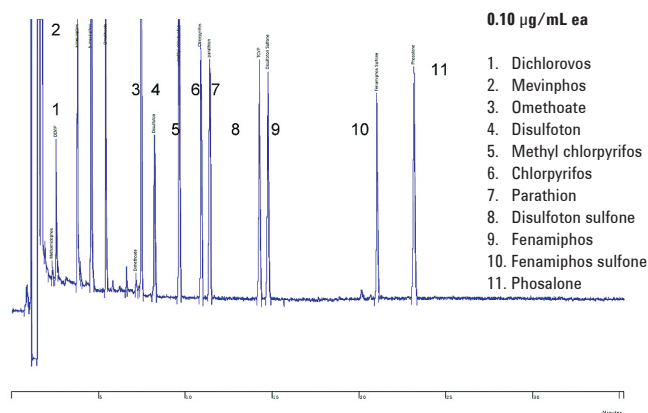


Figure 6. Interference of Sulfur in Broccoli Extract

Phosphorus Sensing Detectors

Figure 7 shows a chromatogram of targeted organophosphorus pesticides being screened in wastewater and sludges by a large water-quality lab. Procedures in EPA methods 1657 and 8141A extraction procedures were followed including liquid-liquid extraction for water and ultrasonic techniques for sludge samples. Sample concentrate was injected via a dual-column injection to two capillary columns interfaced to two PFPDs so that column confirmation could be made easily. The columns used were as follows: 1) Primary column, 0.53 mm x 30 m x 0.5 µm "608" type phase (Agilent equivalent: CP-Sil 8 CB) and 2) Confirmatory column, 0.53 mm x 30 m x 0.5 µm, 100% PDMS, (Agilent equivalent: CP-Sil 5 CB). Figure 7 shows the separation on the "608" type column.

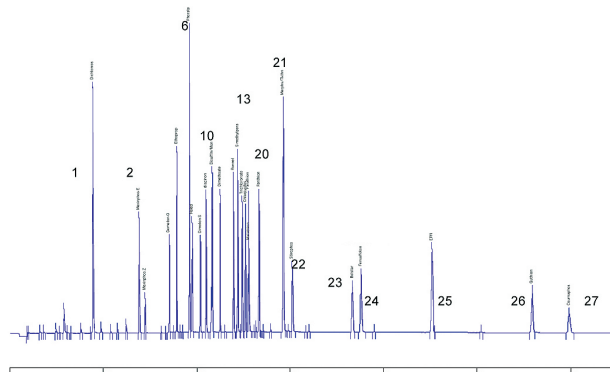


Figure 7. Screening for Organophosphorus Pesticides in Wastewater (courtesy: City of San Diego Wastewater Lab).

The detector linearity of the pesticides was measured over a range of 0.03 to 1 µg/mL. Two of the linearity plots are shown in Figure 9. Table 1 is a tabulation of the relative standard deviations (RSD) of the calibration factors for several other pesticides.

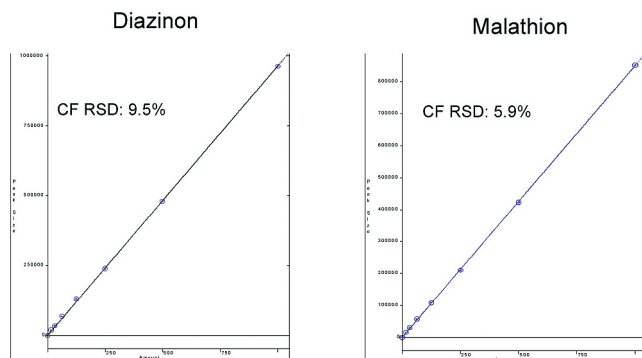


Figure 9. Linearity plots for Diazinon and Malathion from 0.03 to 1.0 µg/mL.

Table 1. Relative Standard Deviations from 0.03 to 1.0 µg/mL for several Organophosphorus Pesticides.

Sample	CF-% RSD	Pesticide	CF-% RSD
Dichlorvos	2.7	Ronnel	6.9
Mevinphos	20	Methyl parathion	2.5
Dimeton	10.4	Trichloronate	2.5
Thimet	3.5	Chlorpyrifos	8.9
Sulfotep	4.0	Parathion	6.6
Naled	5.5	Malathion	4.9
Diazinon	5.3	Fenthion	8.1
Disulfoton	14.1	Guthion (azinphos-methyl)	4.8

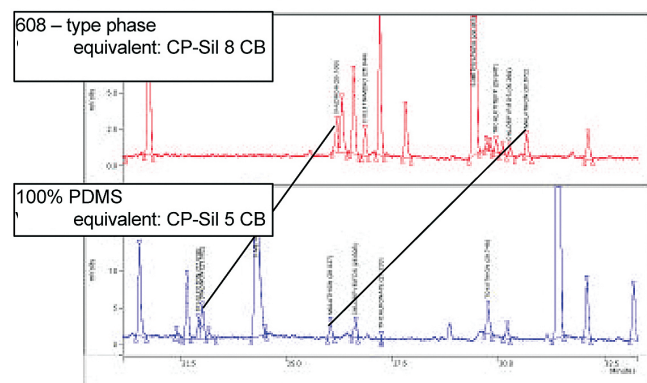


Figure 10. Wastewater Analysis

A dual channel chromatogram of a wastewater sample concentrate is shown in Figure 10. Column confirmation by retention time is apparent for diazinon and malathion, which appear to also have approximately the same peak sizes in the primary and confirmatory columns. Retention time confirmation also is evident for disulfoton and trichloronate. On inspection of the quantitative reports for each PFPD data channel (Figure 11), only the results for diazinon and malathion are comparable on both channels, indicating that they are present in the sample.

PRIMARY COLUMN (DB-608)							
Peak No.	Peak Name	Result (ug/L)	Time (min)	Offset (min)	Area (counts)	Sep. Code	1/2 (sec)
1	DIAZINON	15.97	26.189	-0.001	11905	BV	5.7
2	DISLFTN/MONO	6.79	26.844	0.125	7654	BB	4.3
3	S-METHYL PARA	679.15	29.418	0.039	623504	BB	3.8
4	TRCHLRT/TEPP	2.37	29.947	0.069	2565	BP	3.4
5	CHLORPYRIFOS	3.31	30.269	0.008	2430	VB	0.9
6	MALATHION	8.09	30.672	0.003	5766	BB	3.8
7	MERPHS/TKTHN	1.89	33.510	0.122	1956	BB	0.0
8	STIROPHOS	5.62	33.929	-0.187	3958	BB	5.0
9	BOLSTAR	32.45	39.140	0.089	24666	BB	8.0
10	GUTHION	52.95	55.576	0.163	22508	BB	12.6

CONFIRMATORY COLUMN (DB-1)							
Peak No.	Peak Name	Result (ug/L)	r.t. (min)	Offset (min)	Area (counts)	Sep. Code	1/2 (sec)
1	DISULFOTON	10.67	22.918	0.021	11386	VV	3.8
2	DIAZINON	19.04	23.002	-0.003	18355	VV	5.1
3	S-METHYL PARA	724.35	24.279	0.060	825056	BB	3.7
4	MALATHION	9.68	26.027	-0.003	8238	BB	3.7
5	CHLORPYRIFOS	8.58	26.626	0.196	8549	BB	5.2
6	TRICHLORONATE	0.42	27.233	0.175	399	BB	1.0
7	TORUTHION	23.31	29.749	0.104	18045	BB	4.3

Figure 11. Dual Channel report for primary (DB-608) and confirmatory (DB-1) columns.

Agricultural Products

A dried wheat sample spiked with methyl chlorpyrifos and phosmet and a dried celery sample have both been analyzed by the Luke Method, modified for low moisture, non-fatty products. Samples are blended with acetone/water, filtered and extracted with methylene chloride, dried with Na₂SO₄, and exchanged with acetone. In addition to the two spiked pesticides, malathion was found in the dried wheat sample extract (Figure 12). While peaks appeared to indicate methamidophos, acephate, and malathion in the dried celery sample, only methamidophos was confirmed (Figure 13).

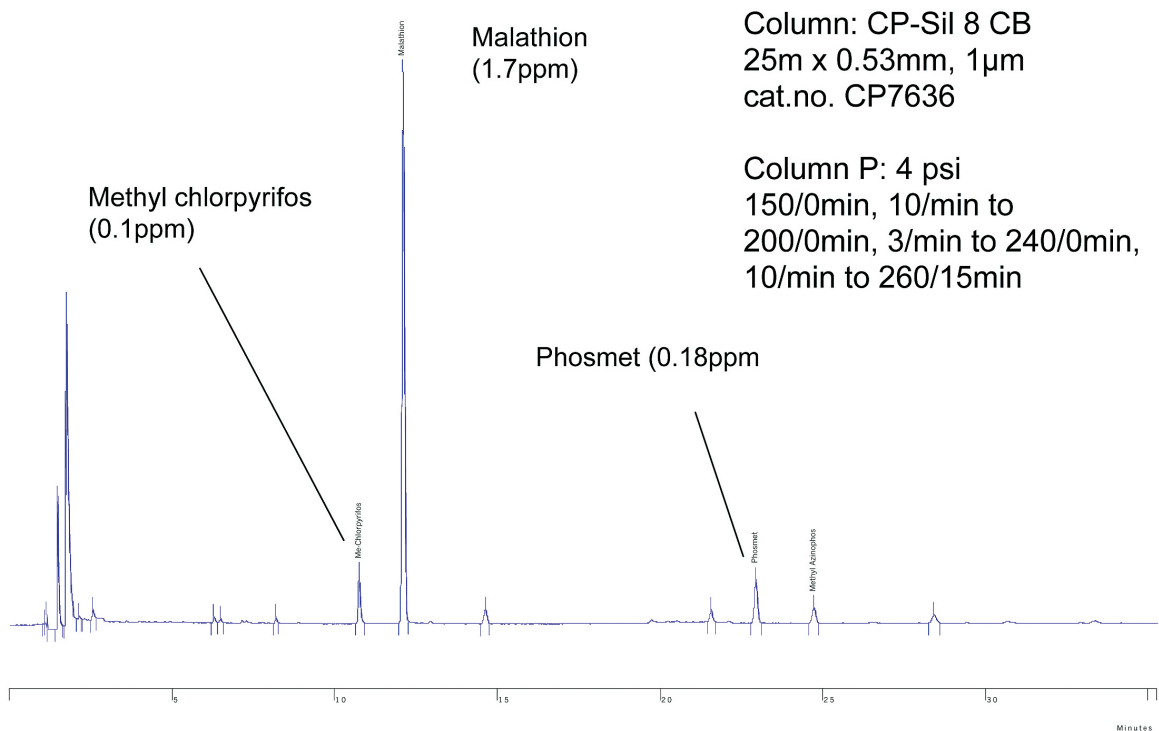


Figure 12. Malathion in Wheat Extract

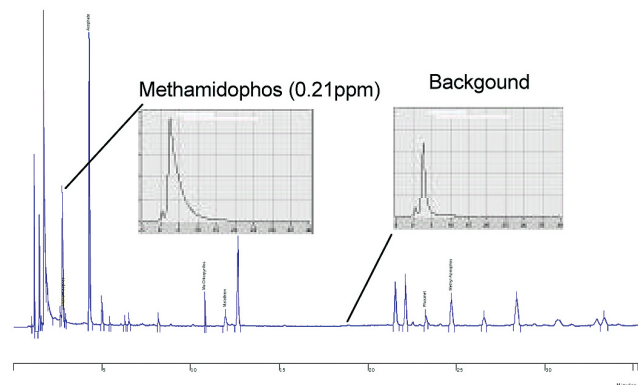


Figure 13. Methamidophos in Dried Celery Extract

Analytical software available for the PFPD permits the analyst to view on screen the emission profiles of the PFPD with a scope like window (Figure 13). This allows the viewing of the emission profile of an eluting peak for qualitative analysis as well as the background emission from the baseline. Methamidophos exhibits the typical P emission profile in Figure 13 and the background window represents only a carbon emission profile from column bleed. The emission profile data from an entire chromatogram can be saved as a data file for subsequent review. The ability to subtract out any sulfur interference is also possible with this software. Finally, the analytical software is helpful in the set up, optimization, and maintenance of the PFPD.

Conclusions

The PFPD is a highly sensitive and selective flame photometric detector capable of detecting a number of elements, 13 of these with infinite selectivity. The PFPD demonstrates excellent linearity, sensitivity and selectivity in the phosphorus mode making it an ideal detector for the determination of organophosphorus pesticides in many matrices.

www.agilent.com/chem

This information is subject to change without notice.

© Agilent Technologies, Inc. 2011

Printed in the USA

31 October, 2011

First published prior to 11 May, 2010

A01608



Agilent Technologies